J. Fluid Mech. (1982), *vol.* 114, *pp.* 443-466
Printed in Great Britain

Modulation by swell of waves and wave groups on the ocean

By P. J. BRYANT

Institute of Geophysics and Planetary Physics, University of California, San Diego†

(Received 13 June 1979 and in revised form 19 February 1981)

Two of the simpler nonlinear wave systems on water of uniform depth are permanent waves and wave groups of permanent envelope. The interaction of each of these wave systems with swell of much smaller amplitude and greater wavelength, propagating in the same direction, is investigated analytically and numerically. A linear-stability analysis of the modulation of these systems by swell shows that they are unstable over short times. Calculations of their evolution over longer times confirms that the initial exponential growth of the modulations is not sustained, and that cyclic recurrence of the modulations occurs in some cases. The modulation of a wave train by swell is found to concentrate the energy of the wave train into single waves in turn, a process which may cause irreversible nonlinear changes such as wave breaking. In contrast, the only observable effect in the modulation of a wave group by swell is a small slow oscillation of the envelope of the group as it propagates. The conclusion is that wave trains on the ocean, generated for example by a wind system of long fetch and duration, disintegrate under the modulation of swell. Wave groups, however, either wind-generated or resulting from the breakdown of wave trains, propagate almost unchanged by the presence of swell.

1. Introduction

The observed regularity in the waves generated on the ocean by a steady wind system suggests that the ocean surface may be modelled locally by a succession of wave groups or even by a periodic wave train. This investigation is directed at the role of swell in the evolution of surface waves and wave groups.

Swell consists of long waves, generated by a remote storm, which are propagating through the wave field. Outside the wave field, the swell propagates with its natural velocity, but on entering the wave field nonlinear interactions not only change slightly the natural velocity of the swell, but also generate side-band modulations to the waves in the wave field. The principal role of the swell in the evolution of the wave field is that of a trigger at small wavenumber generating side-band modulations to waves at the larger wavenumbers within the wave field.

When the small nonlinear interactions between waves balance their linear dispersion, permanent waves and nonlinear wave groups of permanent envelope can exist. Permanent waves are identified with Stokes waves on deeper water and cnoidal waves on shallower water, with a continuous range of wave profiles in between (Bryant 1974). Nonlinear wave groups of permanent envelope are shown below to occur only on deeper water. The evolution, under the initial influence of the side-band modulations caused by swell, of permanent waves and nonlinear wave groups on

† Permanent address: Mathematics Department, University of Canterbury, Christchurch, New Zealand.

water of uniform finite depth, is studied here as a model of the interaction of swell with surface-wave systems on the ocean.

Stokes waves are linearly unstable over short times to side-band modulations in the same direction on deeper water, and linearly stable to these modulations on shallower water (Benjamin 1967; Whitham 1967). Experiments and calculations (Lake *et al.* 1977) have found that in at least some cases cyclic recurrence of the harmonics occurs over longer times. Nonlinear wave groups are linearly unstable over short times to side-band modulations in the same direction on deeper water, and calculations (Bryant 1979) show that in at least some cases cyclic recurrence of the harmonics occurs over longer times.

Cyclic recurrence here means that a nearly cyclic interchange of energy occurs within a dominant set of harmonics for which the nonlinear interactions lie near resonance. The resonance is nearly cyclic, not exactly cyclic, because weaker nonlinear interactions occur with all other harmonics present. Yuen & Ferguson (1978*a*) presented examples (demonstrated below) in which there are two or more competing sets of harmonics having nonlinear interactions near resonance, in which case the cyclic recurrence is obscured. The distinguishing feature in such examples is that the members of these sets of harmonics continue to dominate the wave field, even though a pattern of recurrence cannot be discerned.

Attention has been restricted here, as a first step, to interactions between waves and swell propagating in the same direction. When the waves and swell propagate in different horizontal directions the possibilities increase for competing sets of harmonics, each having nonlinear interactions near resonance. Although cyclic recurrence still occurs in some cases (Yuen & Ferguson 1978*b*), it can be expected that the more common situation is that an interchange of energy occurs within different sets of dominant harmonics, with no discernible overall pattern of recurrence.

The evolution equations for a periodic wave train on water of uniform depth are derived from Laplace's equation, with the appropriate nonlinear surface-boundary conditions, by a perturbation expansion in the amplitude parameter ϵ. Solutions describing permanent waves and nonlinear wave groups are obtained from the evolution equations. Calculations are made of the linear stability of these solutions, with particular attention being given to the unstable modes. A number of representative examples are calculated numerically over long times, these examples being interpreted both in terms of wave evolution and wave-envelope evolution. Conclusions about ocean wave systems are drawn from the calculations.

This approach to nonlinear wave interactions complements the more usual approach by way of model equations such as the Korteweg–de Vries equation, the cubic Schrödinger equation, and their generalizations to two horizontal directions. Although model equations have the advantage of producing solutions and their properties by analytical methods, they have the disadvantage of being based on approximations additional to the small-amplitude approximation. The Korteweg–de Vries equation is valid only for long waves, and the cubic Schrödinger equation for wave groups of narrow wave band. The present method assumes only the small-amplitude approximation, giving it a wider range of validity than model equations, although in most examples it does require the assistance of a computer to obtain solutions. It continues and extends analytical solutions of the model equations, and has fewer approximations than numerical solutions of the model equations.

A subsidiary contribution of this investigation is the determination of the range of nonlinear wave groups of permanent envelope as a function of water depth. As the depth decreases, the shape of the envelope flattens, until at a certain critical depth the family of wave groups tends uniformly to a Stokes wave train. The critical depth is a point of bifurcation between permanent waves and wave groups of permanent envelope, its value being dependent on the wave-slope parameter and on the central wavenumber of the group. These calculations complement those of Hasimoto & Ono (1972), who derived the cubic Schrödinger equation for wave groups on water of finite depth and, from this, solutions corresponding to wave groups of permanent envelope. Although some of their solutions are obtained in § 4, not all of their solutions are physically relevant, for reasons described there.

A new model for nonlinear wind waves has been proposed by Lake & Yuen (1978). They point out that the modulation of a uniform wave train causes the growth of a group structure which has a greater amplitude than the wave train itself because it concentrates locally the energy of the wave train. This property is central to some of the deductions in their model. However, if the structure of the wind-generated ocean surface is that of a succession of groups rather than a uniform wave train, the present calculations show that nonlinear modulation does not necessarily cause a significant increase in the wave amplitude. For this reason, the applicability of their model is dependent on the actual structure of the ocean surface.

2. Governing equations

The water-surface displacement is given the form of a periodic wave train of fundamental wavelength $2\pi l$ modulated in general by a second periodic wave train of larger fundamental wavelength $2\pi L$ in the same direction. The length scale L is taken to be an integer multiple of l in the calculations so that all wavenumbers participating are integer multiples of $1/L$, a simplification which is made for convenience without loss of generality. The mean water depth is h, and the trough-to-crest height of the unperturbed wave train is $2a$. The principal non-dimensional ratios are $\epsilon = a/l$, $\mu = h/l$, and $k_0 = L/l$. The horizontal co-ordinate x and vertical co-ordinate y are measured in units of l from an origin in the mean water surface. Time t is measured in units of $(l/g)^{\frac{1}{2}}$, the surface displacement η in units of a, and the velocity potential ϕ in units of $(gl)^{\frac{1}{2}}a$.

The governing equations in these non-dimensional co-ordinates are

$$\phi_{xx} + \phi_{yy} = 0 \quad (-\mu < y < 0), \tag{2.1a}$$

$$\phi_y = 0 \quad \text{on} \quad y = -\mu, \tag{2.1b}$$

$$\eta_t - \phi_y + \epsilon(\eta\phi_x)_x + \tfrac{1}{2}\epsilon^2(\eta^2\phi_{xy})_x = O(\epsilon^3) \quad \text{on} \quad y = 0, \tag{2.1c}$$

$$\eta + \phi_t + \epsilon\eta\phi_{yt} + \tfrac{1}{2}\epsilon(\phi_x^2 + \phi_y^2) + \tfrac{1}{2}\epsilon^2(\eta^2\phi_{yy})_t + \epsilon^2\eta\eta_{xt}\phi_x = O(\epsilon^3) \quad \text{on} \quad y = 0. \tag{2.1d}$$

The Fourier-series expansions for η and ϕ are

$$\eta = \frac{1}{2}\sum_{k=1}^{\infty} A_k(t) \exp i\left(\frac{kx}{k_0} - \omega_k t\right) + \text{c.c.}, \tag{2.2a}$$

$$\phi = \frac{1}{2}\sum_{k=1}^{\infty} C_k(t) \frac{\cosh\frac{k}{k_0}(y+\mu)}{\cosh\frac{k}{k_0}\mu} \exp i\left(\frac{kx}{k_0} - \omega_k t\right) + \text{c.c.} - \gamma t, \tag{2.2b}$$

where c.c. denotes complex conjugate, and the Fourier amplitudes are slow functions of t. When the Fourier-series expansions for η and ϕ are substituted into (2.1c, d), and only the $O(1)$ terms retained, the linear solution for forward-propagating waves is found to be

$$C_k = -iA_k/\omega_k + O(\epsilon), \tag{2.3a}$$

$$\omega_k = \left(\frac{k}{k_0}\tanh\frac{k\mu}{k_0}\right)^{\frac{1}{2}}. \tag{2.3b}$$

The latter equation for the linear frequency ω_k is taken to be the definition of ω_k, although it is noted that the actual frequency in the presence of nonlinear interactions differs from ω_k.

The Fourier-series expansions for η and ϕ are substituted again into (2.1c, d), with the $O(\epsilon)$ terms now being retained. Equation (2.3a) is used to replace the amplitudes C by the amplitudes A in the $O(\epsilon)$ quadratic terms. A pair of simultaneous first-order differential equations for A_k, C_k is then obtained, from which second-order differential equations for either A_k or C_k alone may be found by elimination. Both equations have the form

$$A_k'' - 2i\omega_k A_k' = \epsilon \times \text{quadratic terms} + O(\epsilon^2),$$

with the complementary function

$$A_k = c_1 + c_2 \exp(2i\omega_k t),$$

where c_1, c_2 are arbitrary constants. Substituting for A_k into the Fourier-series expansion for η (equation 2.2a) then expresses the complementary function as a sum of forward- and backward-propagating waves.

There are general procedures for obtaining first-order differential equations for the evolution of the Fourier amplitudes as a function of nonlinear interactions between waves propagating in all horizontal directions. One such method is that of Watson & West (1975). They derive full evolution equations, but in applying them they ignore terms involving rapidly oscillating exponentials, which are not expected to contribute significantly to the transfer of excitation between wave harmonics. The method used below neglects such terms in the course of the derivation of the evolution equations. It is equivalent to calculating the evolution of the Fourier amplitudes as a function of nonlinear interactions near resonance, with nonlinear interactions far from resonance being neglected.

The initial condition in the present model is that all waves are propagating in the forward x-direction only. The subsequent development is dominated by those nonlinear interactions near resonance. If quadratic interactions are included alone, the only interactions near resonance are those generating forward-propagating waves as the depth-to-wavelength ratio μ decreases towards zero. This is one of the basic implied assumptions of the Korteweg–de Vries equation. Numerical experiments with all quadratic interactions included show that those interactions far from resonance add only rapidly oscillating exponentials to the background of the nearly resonant solutions. For this reason, beginning with (2.3a), backward-propagating waves are ignored, a simplification which achieves a considerable economy in the derivation of the evolution equations and in their solution.

An integrating factor for the second-order differential equations is $\exp(-2i\omega_k t)$. The quadratic terms are divided by $\omega_{k-l} + \omega_l + \omega_k$, $\omega_{k+l} - \omega_l + \omega_k$ on integration, both expressions being $O(1)$ for all positive k and l with the dispersion relation (2.3b). This

is equivalent to the property that backward-propagating waves are far from resonance, The constant of integration (denoted by c_2 above) is put equal to zero because it multiplies backward-propagating waves. The evolution equations for the Fourier amplitudes in terms of quadratic interactions, found by integratior. of the second-order differential equations, are

$$A_k' = \tfrac{1}{4}i\epsilon \sum_{l=1}^{k-1} P_{k,-l} A_l A_{k-l} \exp\left(-i(\omega_{k-l}+\omega_l-\omega_k)t\right)$$
$$+\tfrac{1}{2}i\epsilon \sum_{l=1}^{\infty} P_{k,l} A_l^* A_{k+l} \exp\left(-i(\omega_{k+l}-\omega_l-\omega_k)t\right)+O(\epsilon^2) \quad (k=1,2,\ldots), \quad (2.4a)$$

$$C_k' = \tfrac{1}{4}\epsilon \sum_{l=1}^{k-1} Q_{k,-l} A_l A_{k-l} \exp\left(-i(\omega_{k-l}+\omega_l-\omega_k)t\right)$$
$$+\tfrac{1}{2}\epsilon \sum_{l=1}^{\infty} Q_{k,l} A_l^* A_{k+l} \exp\left(-i(\omega_{k+l}-\omega_l-\omega_k)t\right)+O(\epsilon^2) \quad (k=1,2,\ldots), \quad (2.4b)$$

where A_l^* is the complex-conjugate of A_l. The interaction coefficients P and Q are given in the appendix. It is noted that (2.4*a*, *b*) cannot be integrated directly again because this would involve division by $\omega_{k-l}+\omega_l-\omega_k$, $\omega_{k+l}-\omega_l-\omega_k$, both of which are of a magnitude comparable with ϵ for those k and l near resonance. A first integral of these equations can be found by substituting for either A_k' or C_k' back into the original pair of first-order differential equations for A_k and C_k. It is

$$C_k = -iA_k/\omega_k + \tfrac{1}{4}i\epsilon \sum_{l=1}^{\infty} S_{k,-l} A_l A_{k-1} \exp\left(-i(\omega_{k-l}+\omega_l-\omega_k)t\right)$$
$$+\tfrac{1}{2}i\epsilon \sum_{l=1}^{\infty} S_{k,l} A_l^* A_{k+l} \exp\left(-i(\omega_{k+l}-\omega_l-\omega_k)t\right)+O(\epsilon^2) \quad (k=1,2,\ldots), \quad (2.4c)$$

where $$S_{k,l} = \frac{1}{\omega_k^2}\left(P_{k,l}+\frac{k}{k_0^2}\left(\frac{l}{\omega_l}+\frac{k+l}{\omega_{k+l}}\right)\right), \quad \omega_{-l} = -\omega_l \quad (l>0).$$

This equation is the next-order improvement to (2.3*a*).

The only tertiary interactions to be included in the evolution equations to the next order of magnitude are those for forward-propagating waves which lie near resonance. Resonant quartets for waves propagating in all horizontal directions on deep water are described by Phillips (1974, figure VII. 6). The only quartets to be included here are those with wavenumbers $k, l, m, k+l-m$, where k, l, m lie near a central positive wavenumber. This is one of the basic implied assumptions of the cubic Schrödinger equation. If waves in all horizontal directions are present, there is an increase in the possibilities for resonance consequent on the inclusion of the whole of Phillips' figure instead of only part of it. One such interesting possibility (pointed out by a referee) is the deep-water resonant quartet $(k, k, \frac{9}{4}k, -\frac{1}{4}k)$, $(\omega, \omega, \frac{3}{2}\omega, \frac{1}{2}\omega)$, which places limitations on the present calculations and on the cubic Schrödinger equation. Its effect on the results derived below, when it occurs, is expected to be the generation of an additional set of harmonics in which energy is interchanged, obscuring any cyclic pattern which may have been observable otherwise.

The tertiary-interaction coefficients have been calculated elsewhere by the substitution of the linear relation (2.3*a*) into the $O(\epsilon^2)$ terms of (2.1*c*, *d*), a procedure which is satisfactory on deep water where quadratic interactions are far from resonance.

However, because certain quadratic interactions are retained here for the purpose of applying the evolution equations to waves on shallow water as well as on deep water, the $O(\epsilon)$ contribution of (2.4*c*) to the $O(\epsilon)$ terms of (2.1*c*, *d*) is included for consistency in the present evaluation of the $O(\epsilon^2)$ tertiary interactions. The evolution equations for A_k with the selected tertiary interactions included are found by the same procedure as is described above, and are

$$\begin{aligned} A_k' = {} & \tfrac{1}{4}i\epsilon \sum_{l=1}^{k-1} P_{k,-l} A_l A_{k-l} \exp\left(-i(\omega_{k-l}+\omega-\omega_k)t\right) \\ & + \tfrac{1}{2}i\epsilon \sum_{l=1}^{\infty} P_{k,l} A_l^* A_{k+1} \exp\left(-i(\omega_{k+l}-\omega_l-\omega_k)t\right) \\ & + \tfrac{1}{8}i\epsilon^2 \sum_{l=1}^{\infty} \sum_{m=1}^{k+l-1} R_{k,l,m} A_l^* A_m A_{k+l-m} \exp\left(-i(\omega_m+\omega_{k+l-m}-\omega_l-\omega_k)t\right) \\ & \qquad (k = 1, 2, \ldots), \quad (2.5) \end{aligned}$$

where the interaction coefficient R is given in the appendix. It is noted that

$$R_{k,l,m} = R_{k,l,k+l-m}.$$

The only independent check that could be devised on the accuracy of these coefficients was that they should give the correct parameters for Stokes waves on water of finite depth, a check described in § 3.

Resonance occurs when a frequency triad or quartet in one of the above exponentials is zero. The frequency triads are never zero in the gravity-wave range, but the quartets are zero or nearly zero when the wavenumbers lie within a narrow wave band. If such a wave band is centred on wavenumber k_0, the above quartet may be rewritten

$$\omega_m+\omega_{k+l-m}-\omega_l-\omega_k = (k-m)(l-m)\left(\frac{d^2\omega}{dk^2}\right)_{k_0} + O\left(\frac{k-k_0}{k_0}\right)^3. \quad (2.6)$$

The dominant contribution from the tertiary interactions occurs therefore for wavenumbers $m = k$, $m = l$, and has the form

$$\tfrac{1}{4}i\epsilon^2 \sum_{l=1}^{\infty} R_{k,l,l} A_l^* A_l A_k. \quad (2.7)$$

This contribution is proportional to A_k, implying that it is equivalent to a nonlinear correction to the linear frequency ω_k, which now becomes (from (2.2*a*))

$$\omega_k - \tfrac{1}{4}\epsilon^2 \sum_{l=1}^{\infty} R_{k,l,l} A_l^* A_l. \quad (2.8)$$

It will be shown in § 5 how the eigenvalues calculated from a linear-stability analysis of solutions of (2.5) may be identified with these nonlinear frequencies.

3. Permanent waves

Permanent waves on water of uniform depth are described by a surface displacement

$$\eta = \sum_{k=1}^{\infty} a_k \cos k(x-ct), \quad (3.1a)$$

where a_k ($k = 1, 2, \ldots$) and c are calculated as functions of ϵ and μ. It follows from (2.2a) that

$$A_k = a_k \exp i(\omega_k - kc)t \quad (k = 1, 2, \ldots), \tag{3.1b}$$

with $k_0 = 1$, so that (2.5) become

$$(\omega_k - kc)\, a_k = \tfrac{1}{4}\epsilon \sum_{l=1}^{k-1} P_{k,-l} a_l a_{k-l} + \tfrac{1}{2}\epsilon \sum_{l=1}^{\infty} P_{k,l}\, a_l\, a_{k+l} + \tfrac{1}{8}\epsilon^2 \sum_{l=1}^{\infty} \sum_{m=1}^{k+l-1} R_{k,l,m} a_l\, a_m a_{k+l-m} \quad (k = 1, 2, \ldots). \tag{3.2a}$$

The geometric relation consequent on the definition of ϵ is

$$\sum_{l=1}^{\infty} a_{2l-1} = 1. \tag{3.2b}$$

Stokes waves are such that $a_2/a_1 = O(\epsilon)$, $a_3/a_2 = O(\epsilon)$. Equations (3.2a) may then be written

$$(\omega_1 - c)\, a_1 = \tfrac{1}{2}\epsilon P_{1,1} a_1 a_2 + \tfrac{1}{8}\epsilon^2 R_{1,1,1} a_1^3 + O(\epsilon^4), \quad (\omega_2 - 2c)\, a_2 = \tfrac{1}{4}\epsilon P_{2,-1} a_1^2 + O(\epsilon^3),$$

and have the solution

$$a_1 = 1 + O(\epsilon^2), \tag{3.3a}$$

$$a_2 = \frac{\epsilon P_{2,-1}}{4(\omega_2 - 2\omega_1)} + O(\epsilon^3), \tag{3.3b}$$

$$c = \omega_1 - \tfrac{1}{8}\epsilon^2 \left(R_{1,1,1} + \frac{P_{1,1} P_{2,-1}}{\omega_2 - 2\omega_1} \right) + O(\epsilon^4). \tag{3.3c}$$

When the values for the interaction coefficients are substituted and the expressions simplified, Stokes' solution (Whitham 1974, pp. 474–475) is obtained.

Cnoidal waves on shallow water are such that the harmonics approximate a geometric sequence with ratio r, where r tends towards 1 from below as al^2/h^3 increases (Bryant 1974, § 3). The increase in the number of harmonics makes analytical solutions of (3.2) tedious to calculate. Numerical solutions are easy to calculate, the method used being to find the solution for a number N of harmonics, then to increase N step by step until a prescribed numerical precision is obtained. The generalized Newton–Raphson method is quick and efficient for this purpose.

The use of numerical methods allows permanent-wave solutions of (2.5) to be calculated as continuous functions of ϵ and μ. The solutions approximate Stokes waves on deeper water and cnoidal waves on shallower water, and comprise part of the set of solutions whose properties under modulation are investigated below.

4. Wave groups of permanent envelope

Nonlinear wave groups of permanent envelope on water of uniform depth are described by the surface displacement

$$\eta = \frac{1}{2} \sum_{k=1}^{k_{02}} a_k \exp i \frac{k}{k_0}(x - ct) + \frac{1}{2} \left(\sum_{k=k_{11}}^{k_{12}} a_k \exp i \frac{k - k_0}{k_0}(x - ct) \right) \exp\{i(x - \omega_{k_0} t) - i\alpha\epsilon^2 t\} + \frac{1}{2} \left(\sum_{k=k_{21}}^{k_{22}} a_k \exp i \frac{k - 2k_0}{k_0}(x - ct) \right) \exp\{2i(x - \omega_{k_0} t) - 2i\alpha\epsilon^2 t\} + \ldots + \text{c.c.} \tag{4.1}$$

The principal spectral contribution to the wave group is from the wave band centred on k_0, the second sum in the description above. Quadratic interactions within this wave band generate subsidiary contributions from wavenumbers near 1, and from wave bands centred on $2k_0, 3k_0, \ldots$. The physical interpretation of this description is that of a wave group whose envelope propagates with velocity c (the group velocity at wavenumber k_0), inside which is a wave of frequency $\omega_{k_0} + \alpha\epsilon^2$, where α is to be calculated. It is the generalization of the description used previously (Bryant 1979, § 3) consequent on the inclusion of quadratic interactions.

If the water surface is to have the description of (4.1), the Fourier amplitudes must be given by

$$A_k = \begin{cases} a_k \exp i\left(\omega_k - \dfrac{kc}{k_0}\right)t \quad (1 \leqslant k \leqslant k_{02}), \\ a_k \exp i\left(\omega_k - \omega_{k_0} - \dfrac{k-k_0}{k_0}c - i\alpha\epsilon^2\right)t \quad (k_{11} \leqslant k \leqslant k_{12}), \\ a_k \exp i\left(\omega_k - 2\omega_{k_0} - \dfrac{k-2k_0}{k_0}c - 2i\alpha\epsilon^2\right)t \quad (k_{21} \leqslant k \leqslant k_{22}), \\ \vdots. \end{cases} \tag{4.2a}$$

The parameter ϵ is defined from the principal wave band alone by

$$\sum_{k=k_{11}}^{k_{12}} a_k = 1. \tag{4.2b}$$

The central wavenumber k_0 is fixed by choosing c to be the group velocity for this wavenumber. The set of equations obtained by substituting (4.2a) into (2.5), together with (4.2b), is then solved for the complete set of harmonics a_k and the frequency correction α. The wave-band limits $k_{02}, k_{11}, k_{12}, k_{21}, k_{22}, \ldots$ are increased step-by-step until solutions are obtained to a prescribed precision. The computational effort is reduced considerably by including only the tertiary interactions between harmonics in each of the wave bands, and not the tertiary interactions between harmonics in different wave bands. This simplification is suggested by the property that the tertiary interactions are significant only for harmonics within a narrow waveband (cf. (2.6)). Calculations with and without this simplification confirm its validity and efficiency.

Nonlinear wave-group solutions were calculated for a range of values of ϵ, μ and k_0, and were added to the set of solutions whose properties under modulation are investigated below. The effect of changing depth is illustrated in figure 1. As the depth decreases, the envelope of the wave group flattens, until the wave group tends towards a uniform train of permanent waves. The point of bifurcation between permanent waves and nonlinear wave groups is dependent on ϵ and k_0. For the values in figure 1 ($\epsilon = 0{\cdot}1$, $k_0 = 10$) bifurcation occurs at $\mu = 1{\cdot}55$.

The structure of nonlinear wave groups on deep water may be described as being due to a balance between the second-order Stokes amplitude correction to the wave speed (Whitham 1974, equation (13.123)) and the weak dispersion. If dispersion is considered alone, a wave group must gradually disintegrate as the longer waves composing it have a greater group velocity than the shorter waves. The effect of the Stokes correction is that of a positive mean velocity maximum under the centre of the group, with a region of mean velocity convergence forward of the centre and mean velocity divergence behind the centre. The longer waves are therefore shortened and their group velocity

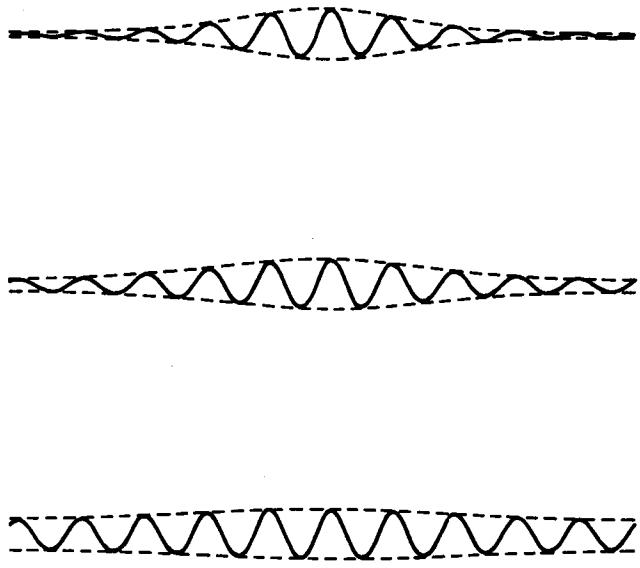

FIGURE 1. One group wavelength of nonlinear wave groups of permanent envelope, $\epsilon = 0{\cdot}1$, $k_0 = 10$, at the depth ratios $\mu = 5, 3, 1{\cdot}75$. The dashed curves are the envelopes, and the solid curves are the water-surface displacement at an instant. (Horizontal contraction 8π.)

reduced as they move ahead of the centre, with the reverse occurring for the shorter waves which fall behind the centre. The overall effect of the Stokes amplitude correction is therefore to counteract the weak dispersion, allowing the occurrence of wave groups of permanent envelope. As the water depth becomes less, a second-order uniform mean flow occurs with a negative maximum under the centre of the group (Whitham 1974, § 16.9). This reduces the ability of the Stokes amplitude correction to balance the dispersion, until at the point of bifurcation described above a balance is no longer possible and wave groups of permanent envelope cannot occur.

Hasimoto & Ono (1972) derived the cubic Schrödinger equation for the envelope of nonlinear wave groups on water of finite depth, showing that the coefficient of the cubic term changes sign at non-dimensional depth $\mu = 1{\cdot}363$. They obtained solutions of permanent envelope which have the elliptic dn form when $\mu > 1{\cdot}363$, and the elliptic sn form when $\mu < 1{\cdot}363$. The envelopes sketched in figure 1 agree qualitatively with the dn solutions, but the sn solutions when $\mu < 1{\cdot}363$ could not be found. The mathematical reason for the failure of their solutions in this range is that the envelope is described by $|\mathrm{sn}|$, not by sn, and the $|\mathrm{sn}|$ function is not a solution of the cubic Schrödinger equation because sn changes sign within each wavelength. The physical reason for the failure is that the second-order uniform mean flow described in the previous paragraph increases as the depth decreases, and cannot be balanced to produce an envelope of permanent form at shallow depths.

5. Linear stability

The linear stability of permanent waves and nonlinear wave groups is now investigated. Small perturbations are applied to the set of solutions calculated in § 3 and § 4, and the resulting linear evolution equations for the perturbations are solved

with the assistance of linear-algebra routines on a computer (Wilkinson & Reinsch 1971).

The previous description of a permanent wave (3.1 a) is now modified by setting the fundamental wavenumber equal to $k_0 (= L/l)$. Side-band modulations at wavenumbers $k_0 \pm 1$ are introduced when the perturbed permanent wave is described by

$$\eta = \tfrac{1}{2}\hat{B}(1,t)\exp i\{(1/k_0)(x-ct)\} + \frac{1}{2}\sum_{n=1}^{\infty}[\hat{B}(nk_0-1,t)\exp i\{(n-1/k_0)(x-ct)\} + a_n \exp in(x-ct) + \hat{B}(nk_0+1,t)\exp i\{(n+1/k_0)(x-ct)\}] + \text{c.c.} \quad (5.1)$$

It should be noted that the amplitudes $\hat{B}$ are amplitudes in a frame of reference moving with velocity c, which although small in magnitude do have strong dependence on t. The amplitude $\hat{B}(1,t)$, for example, contains a contribution to η representing the swell slightly forced from its natural velocity, together with modulation contributions generated by nonlinear interactions. The physical description here is of a permanent wave with wavenumbers nk_0 and amplitudes a_n, $n = 1, 2, \ldots$, interacting with swell of wavenumber 1 at much smaller amplitude, causing a time variation in the swell amplitude as well as triggering side-band modulations at wavenumbers $nk_0 \pm 1$, $n = 1, 2, \ldots$. The linearization in the small amplitude of the swell means that the side-band modulations at wavenumbers $nk_0 \pm 2$, $nk_0 \pm 3, \ldots$ are neglected because they are proportional to higher products of the swell amplitude. Although this linearization is valid initially, it may not be valid over longer times, to be investigated separately (§ 6).

The evolution equations for the perturbed Fourier amplitudes are found by substitution of the harmonics from the above description into (2.5), followed by linearization in $\hat{B}$. The set of first-order linear differential equations may be rearranged to describe the dependent variables $\hat{B}(nk_0+1)$, $n = 0, 1, 2, \ldots$, and $\hat{B}^*(nk_0-1)$, $n = 1, 2, 3, \ldots$, as functions of ϵt. Solutions are sought for which each $\hat{B}$ has the time dependence $\exp(i\lambda\epsilon t)$, with the number of values of n being increased step-by-step until the eigenvalues converge to within a prescribed precision. Linear instability is associated with the occurrence of complex-conjugate pairs of values for λ. The set of equations and the method of solution are generalizations of those described previously (Bryant 1974, § 4).

The stability diagram for permanent waves at a given wave steepness $\epsilon = 0{\cdot}1$, as a function of the depth ratio μ, is presented in figure 2. The minimum value of μ at which instability occurs is 1·35, in close agreement with the value 1·36 calculated in the limit as ϵ tends to zero (Whitham 1974, § 16.11). The cross-section of figure 2 at $\mu = 5$, the imaginary part of the eigenvalues, is drawn in figure 3 (a). The real part of the eigenvalues at $\mu = 5$ is drawn in figure 3 (b), splitting into two distinct real eigenvalues in the stable section of the range of l/L. It is of interest that the transition from instability to stability is of the same form as that calculated by Longuet-Higgins (1978), for example in his figures 1 and 2. His calculations were made at constant $l/L = \frac{1}{2}$ and constant $\mu = \infty$ as a function of ϵ. The present calculations illustrated in figures 3 (a, b) describe the transition at constant $\epsilon = 0{\cdot}1$ and constant $\mu = 5$ as a function of l/L. The two eigenvalues in the stable section of the range are associated with the two side-band modulations at wavenumbers $k_0 \pm 1$. This association is explored now in more detail.

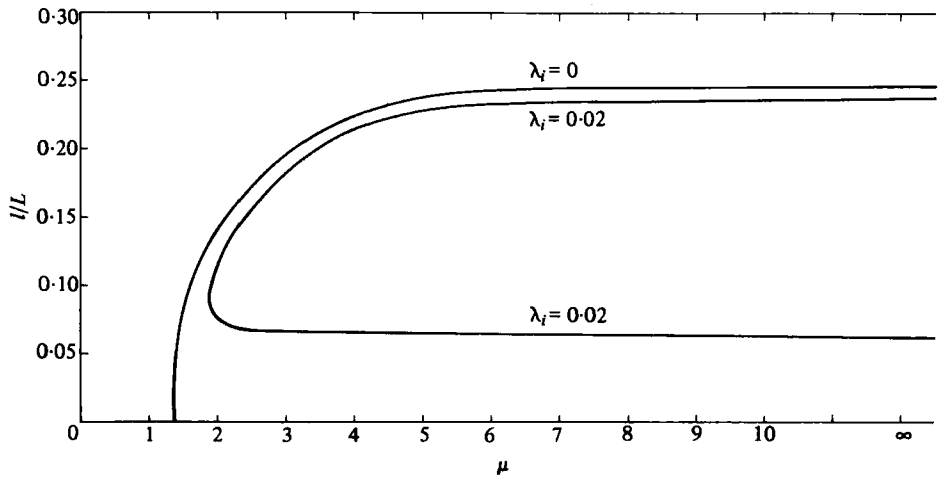

FIGURE 2. The stability diagram for permanent waves, $\epsilon = 0{\cdot}1$, as a function of the depth ratio μ and the fundamental-to-swell wavelength ratio l/L. The outer curve is the instability boundary $\lambda_i = 0$, and the inner curve is the contour of constant growth rate $\lambda_i = 0{\cdot}02$.

The nonlinear frequency of the perturbation at wavenumber $k_0 - 1$ is, from (2.8),

$$\omega_{k_0-1} - \tfrac{1}{4}\epsilon^2 \sum_{n=1}^{\infty} R_{k_0-1,\,k_0 n,\,k_0 n} a_n^2.$$

If further nonlinear contribution is negligible, the associated eigenvalue is, from (5.1),

$$\Omega_{k_0-1} = [(1 - 1/k_0)\,c - \omega_{k_0-1}]/\epsilon + \tfrac{1}{4}\epsilon \sum_{n=1}^{\infty} R_{k_0-1,\,k_0 n,\,k_0 n} a_n^2, \tag{5.2a}$$

and, for wavenumber $k_0 + 1$,

$$\Omega_{k_0+1} = [(1 + 1/k_0)\,c - \omega_{k_0+1}]/\epsilon + \tfrac{1}{4}\epsilon \sum_{n=1}^{\infty} R_{k_0+1,\,k_0 n,\,k_0 n} a_n^2. \tag{5.2b}$$

The two estimated eigenvalues are drawn in figure 3(*c*).

The agreement between the calculated and estimated eigenvalues in figures 3(*b*, *c*) respectively is good, with the estimated eigenvalues coalescing into a complex-conjugate pair when they are sufficiently close. The nonlinear frequencies derived originally in (2.8) do provide a good estimate of the frequencies of the perturbations after modification by the permanent wave. The estimated eigenvalues in (5.2) are identified with these nonlinear frequencies relative to the permanent wave. Instability is associated with the nonlinear frequencies of pairs of side-band modulations being sufficiently close in the frame of reference of the permanent wave. These conclusions are the generalization to a permanent wave composed of any number of harmonics of the reasons advanced by Phillips (1974, pp. 207–211) for the linear instability of a Stokes wave composed of two harmonics.

Nonlinear wave groups of permanent envelope were found to be linearly unstable over the whole parameter range investigated. Previous calculations (Bryant 1979) at large values of k_0 on water of infinite depth, and the present calculations on perturbations of the extended wave-group description (4.1) at smaller values of k_0 on water of finite depth, all displayed instability. The margin of instability was found to be much smaller than that for side-band modulation of a permanent wave train, the

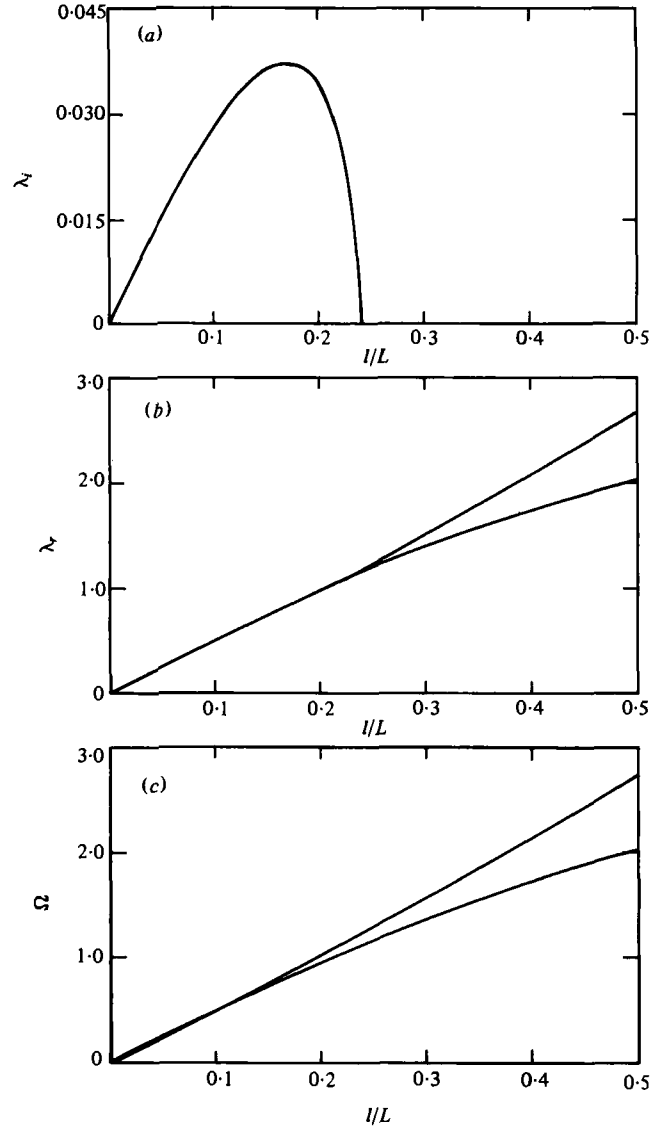

FIGURE 3. (*a*) The imaginary part of the calculated complex eigenvalues for the permanent wave, $\epsilon = 0{\cdot}1$, $\mu = 5$, equivalent to the cross-section of figure 2 at $\mu = 5$. (*b*) The real part of the calculated complex eigenvalues, $0 \leqslant l/L < 0{\cdot}24$, and the lowest calculated eigenvalue pair, $0{\cdot}24 \leqslant l/L \leqslant 0{\cdot}5$. (*c*) The estimated eigenvalues (5.2).

stability being almost neutral. The association between the calculated eigenvalues and the eigenvalues estimated from the nonlinear frequencies is now explored.

The dominant spectral contribution to the wave group is from the wave band centred on k_0, with subsidiary contributions from wavenumbers near 1 and wave bands centred on $2k_0$, $3k_0$, ... The wave group is modulated in the present calculations at side-band wavenumbers $k_0 - 1$ and $k_0 + 1$, two wavenumbers already present in the wave group. The linear-stability analysis must be applied therefore to perturbations of all the harmonics in the wave group, in exactly the same manner as if the pertur-

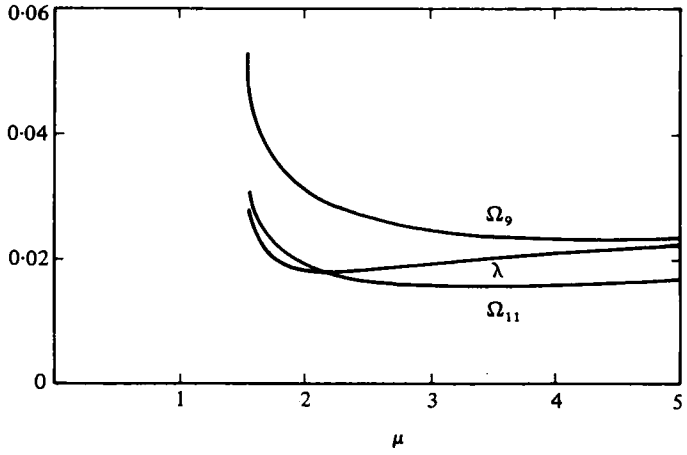

FIGURE 4. The lowest calculated real eigenvalue λ and the estimated side-band eigenvalues Ω_9, Ω_{11} for the nonlinear wave group, $\epsilon = 0{\cdot}1$, $k_0 = 10$, as a function of the depth ratio μ.

bation were that of swell at wavenumber 1. The nonlinear frequency of the perturbation to the harmonic at wavenumber k is, from (2.8),

$$\omega_k - \tfrac{1}{2}\epsilon^2 \sum_n R_{k,n,n} a_n^2.$$

The estimated eigenvalues associated with wavenumbers $k_0 - 1$, k_0, $k_0 + 1$ are therefore, from (4.1),

$$\Omega_{k_0-1} = [\omega_{k_0} - c/k_0 + \alpha\epsilon^2 - \omega_{k_0-1}]/\epsilon + \tfrac{1}{2}\epsilon \sum_n R_{k_0-1,n,n} a_n^2, \tag{5.3a}$$

$$\Omega_{k_0} = \alpha\epsilon + \tfrac{1}{2}\epsilon \sum_n R_{k_0,n,n} a_n^2, \tag{5.3b}$$

$$\Omega_{k_0+1} = [\omega_{k_0} + c/k_0 + \alpha\epsilon^2 - \omega_{k_0+1}]/\epsilon + \tfrac{1}{2}\epsilon \sum_n R_{k_0+1,n,n} a_n^2. \tag{5.3c}$$

The dependent variables in the stability analysis are $\hat{B}_k$, $\hat{B}_k^*$, for all wavenumbers k in the original wave group. The real eigenvalues occur therefore in pairs of equal magnitude and opposite sign, while the complex eigenvalues occur in the double pair $\pm\lambda_r \pm i\lambda_i$. When the estimated eigenvalues are matched with the calculated eigenvalues, it is found that the six central estimated eigenvalues $\pm\Omega_{k_0-1}$, $\pm\Omega_{k_0}$, $\pm\Omega_{k_0+1}$ are associated with the four calculated complex eigenvalues and the smallest pair of calculated real eigenvalues. The smallest calculated real eigenvalue λ is compared with Ω_9 and Ω_{11} in figure 4 for wave groups of central wavenumber 10, as a function of the depth ratio μ. Both λ_r and λ_i are of magnitude about 10^{-4} in the double pairs of calculated complex eigenvalues. It appears that the complex eigenvalues are associated with Ω_{k_0} and $\frac{1}{2}(\Omega_{k_0-1} - \Omega_{k_0+1})$, while the smallest pair of real eigenvalues is associated with $\frac{1}{2}(\Omega_{k_0-1} + \Omega_{k_0+1})$.

The corresponding physical mechanism of instability may be as follows. The perturbation to the central harmonic with wavenumber k_0 propagates under the influence of all harmonics at a velocity almost equal to that of the central harmonic itself. Near-resonant transfer of energy can take place, and the perturbation grows exponentially. At the same time, the perturbations to the two side-band harmonics

with wavenumbers k_0-1, k_0+1, when superposed, propagate with a velocity sufficiently close to that of the central harmonic that near-resonant transfer of energy causes their exponential growth also. In contrast with a periodic wave train, the harmonics of the nonlinear wave groups are already in a state of balance between the central and side-band wavenumbers, resulting in the perturbations to the side-band harmonics having much smaller growth rates than the side-band modulations to a periodic wave train.

6. Evolution equations

The linear-stability analysis of § 5 describes the initial evolution of a modulated wave or wave group. The evolution over longer times is determined by numerical solution of the evolution equations (2.5).

A modulated permanent wave train is represented by the surface displacement

$$\eta = \frac{1}{2}\sum_{k=1}^{\infty} B_k(t)\exp i\frac{k}{k_0}(x-ct)+\text{c.c.}, \tag{6.1a}$$

where

$$B_k(t) = A_k(t)\exp i\left(\frac{kc}{k_0}-\omega_k\right)t \quad (k=1,2,\ldots), \tag{6.1b}$$

and c is the velocity of the unmodulated permanent wave. Equations (2.5) then become

$$B_k'-i\left(\frac{kc}{k_0}-\omega_k\right)B_k = \tfrac{1}{4}i\epsilon\sum_{l=1}^{k-1}P_{k,-l}B_lB_{k-l}+\tfrac{1}{2}i\epsilon\sum_{l=1}^{\infty}P_{k,l}B_l^*B_{k+l} + \tfrac{1}{8}i\epsilon^2\sum_{l=1}^{\infty}\sum_{m=1}^{k+l-1}R_{k,l,m}B_l^*B_mB_{k+l-m} \quad (k=1,2,\ldots). \tag{6.2}$$

This set of differential equations is converted to the set of difference equations

$$\frac{B_k(\epsilon t+\epsilon\Delta t)-B_k(\epsilon t-\epsilon\Delta t)}{2i\epsilon\Delta t}-\frac{1}{2\epsilon}\left(\frac{kc}{k_0}-\omega_k\right)(B_k(\epsilon t+\epsilon\Delta t)+B_k(\epsilon t-\epsilon\Delta t)) = \frac{1}{4}\sum_{l=1}^{k-1}P_{k,-l}B_l(\epsilon t)\,B_{k-l}(\epsilon t)+\frac{1}{2}\sum_{l=1}^{\infty}P_{k,l}B_l^*(\epsilon t)\,B_{k+l}(\epsilon t) + \tfrac{1}{8}\epsilon\sum_{l=1}^{\infty}\sum_{m=1}^{k+l-1}R_{k,l,m}B_l^*(\epsilon t)\,B_m(\epsilon t)\,B_{k+l-m}(\epsilon t) \quad (k=1,2,\ldots). \tag{6.3}$$

These equations are integrated step-by-step from the initial conditions for the modulated permanent wave.

The computational effort required to calculate the tertiary interactions was reduced considerably by making the same simplification as was described in § 4. This consisted in including the tertiary interactions between harmonics within each of the wave bands centred on $k_0, 2k_0, \ldots$, and that bounded by 1, but not including the tertiary interactions between harmonics in different wave bands. Calculations over long times with and without this simplification showed no significant difference in the solutions obtained, but a considerable improvement in computation time.

The representation used to describe the evolution of a modulated nonlinear wave group is the same as that of (4.1) except that the constant amplitudes a_k are replaced by time-dependent amplitudes $B_k(t)$. It is implicit in this representation that the

modulation to the wave group is made at one of the wavenumbers already present in the group. Modulations at other wavenumbers have been found previously to yield no new properties (Bryant 1979). The set of difference equations used for the numerical calculations are of similar form to (6.3), and the same simplification in the calculation of the tertiary interactions was made here also.

In §§ 7–9, a number of examples are presented of the evolution over long times of modulated waves and wave groups. A common feature of these examples is the small initial amplitude of the modulation, about 1 % of the amplitude of the unmodulated wave or wave group. This corresponds to the interaction of background ocean swell with the ocean surface wave field. The interaction of swell of wavenumber 1 with a wave train of fundamental wavenumber $k_0 (\gg 1)$ generates side-band harmonics at wavenumbers $k_0 \pm 1$. These then interact resonantly with the fundamental, with the original modulation at wavenumber 1 having only a passive role. For this reason, the initial modulation in the examples following is chosen to occur directly at the side-band wavenumbers $k_0 \pm 1$. It was found that, when the initial modulation was applied at the swell wavenumber 1, the only difference was that the initial growth of the side-band harmonics was flatter than that illustrated in the examples following.

7. Modulated Stokes wave: cyclic recurrence

The first example to be presented is one with good cyclic recurrence. The Stokes wave with parameters $\epsilon = 0{\cdot}1$, $\mu = 5$ is modulated at 5 times the fundamental wavelength ($l/L = 0{\cdot}2$). This modulation is seen from figure 3 to be unstable, with a growth rate near the maximum for the wave. Using the notation defined in § 5, the fundamental has wavenumber 5, with the initial side-band modulation applied at wavenumbers 4 and 6. The initial conditions used for the numerical integration are $B_4 = 0{\cdot}01$, $B_5 = 0{\cdot}9958$, $B_6 = 0{\cdot}01$, $B_{10} = 0{\cdot}0503$, $B_{15} = 0{\cdot}0041$, $B_k = 0$ otherwise; $1 \leqslant k \leqslant 16$, with $c = 1{\cdot}00497$.

The moduli of the Fourier amplitudes B_4, B_5, B_6 are drawn in figure 5(*a*) together with the linearized solutions calculated by the methods of § 5. The cyclic recurrence has a period of about $\epsilon t = 88\pi$. The initial agreement between the linearized solution and the full solution is good while $|B_4|$ and $|B_6|$ are less than about 0·25. The linearized solution then continues to grow exponentially, while the full solution attains a maximum value and returns close to its initial value.

The surface displacement is illustrated in two ways. In figure 5(*b*) the surface displacement itself is shown in a frame of reference moving with the phase velocity c of the unmodulated Stokes wave. The interesting feature of this figure is the interval in the centre of the cycle of recurrence where the side-band harmonics have maximum values, causing the wave profile to change more rapidly than elsewhere, with individual crests rising to larger amplitudes. This is the interval where irreversible nonlinear processes such as wave subsidence or wave breaking would occur for sufficiently large values of ϵ, the steepness of the unmodulated wave. The initial modulation of only about 1 % of the Stokes-wave amplitude concentrates energy from the 5 waves of the modulation wavelength into single waves in turn. It may be noted also that there is an advance in phase of the uniform wave train between the two sides of this central interval.

The upper side of the envelope of the surface displacement is shown in figure 5(*c*) in

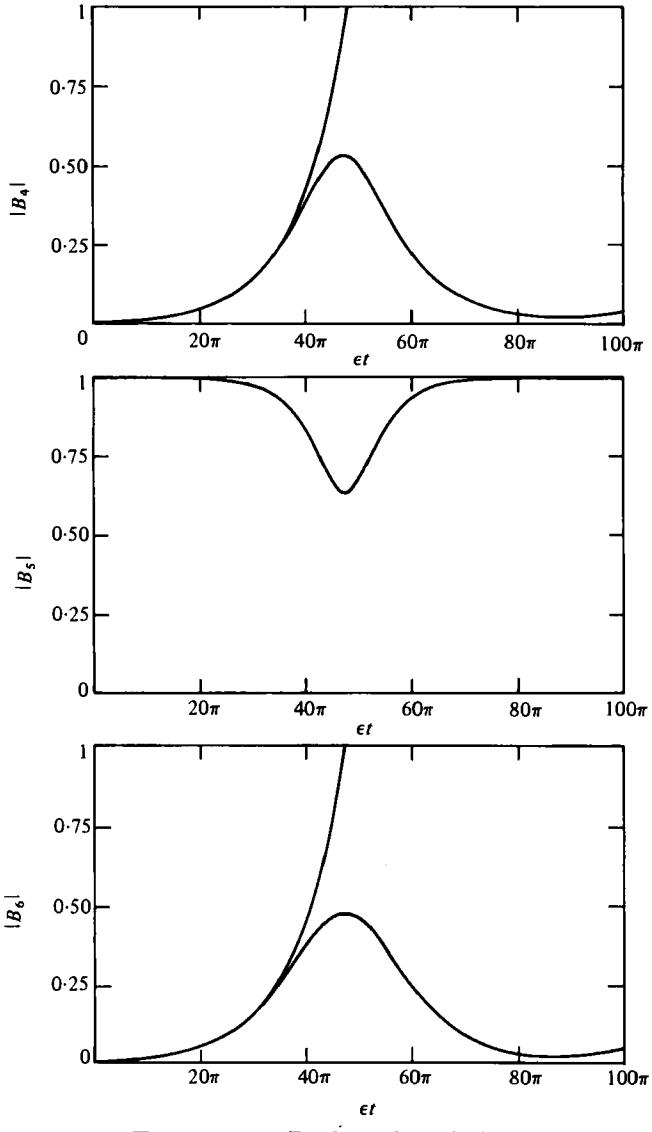

FIGURE 5 (*a*). For legend see facing page.

a frame of reference moving with the group velocity of the fundamental harmonic $k_0 = 5$. The initial cross-section covers the same ten wavelengths as in figure 5 (*b*), with the modulation being a maximum at $x = 0$ and at $x = 10\pi$. The ridges in the central interval of the cycle of recurrence originate from the initial maxima in the modulation. These ridges propagate with a velocity in excess of the group velocity of the fundamental harmonic. Yuen & Ferguson (1978*a*) integrated the cubic Schrödinger equation from initial conditions of the same form but with a larger modulation than that used here. The results of their calculations (figure 1 (*a*) of their paper) are qualitatively the same as those illustrated in figure 5 (*c*).

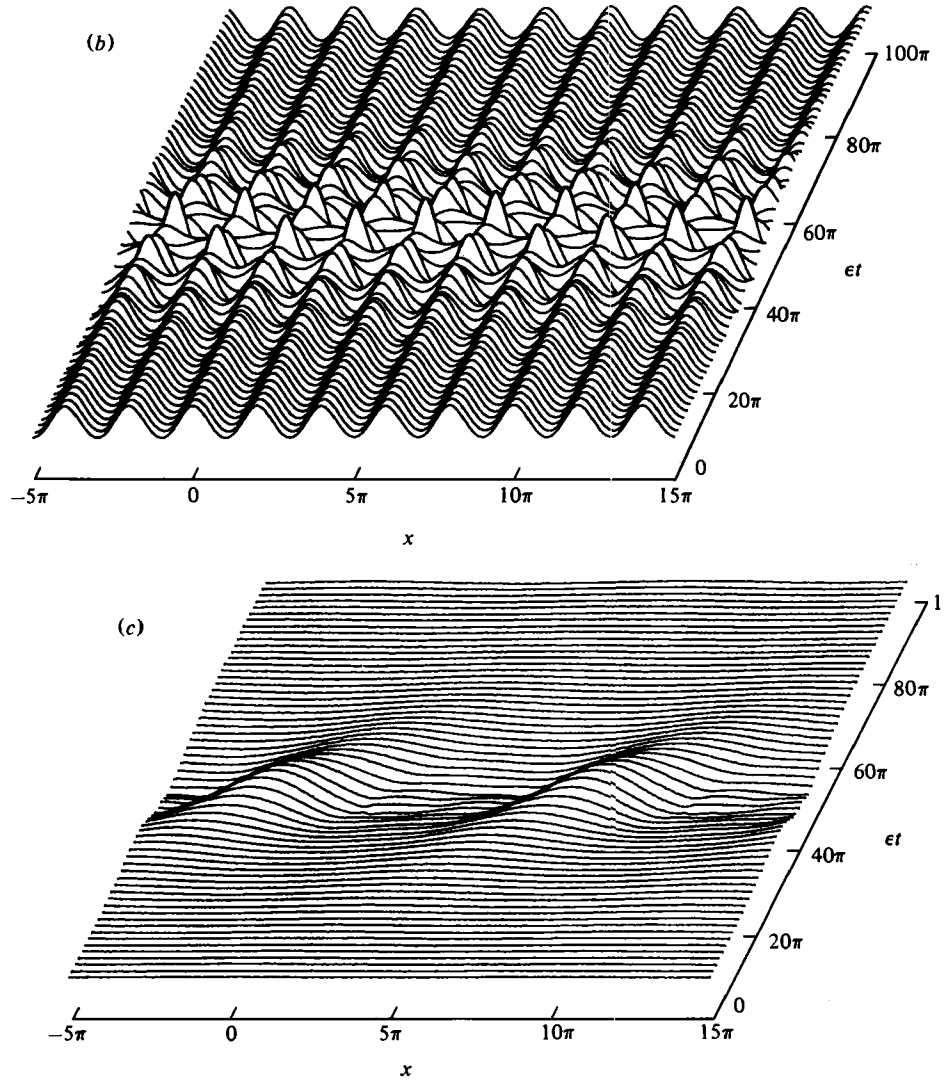

FIGURE 5. (*a*) Moduli of the Fourier amplitudes B_4, B_5, B_6 for the modulated permanent wave, $\epsilon = 0{\cdot}1$, $\mu = 5$, $l/L = 0{\cdot}2$. The upper curves for B_4 and B_6 are the solutions calculated by the linear-stability analysis of § 5. (*b*) Cross-sections of the water-surface displacement at intervals $\epsilon t = 1{\cdot}6\pi$, in a frame of reference moving with the wave velocity, for two modulation wavelengths of the modulated permanent wave $\epsilon = 0{\cdot}1$, $\mu = 5$, $l/L = 0{\cdot}2$. (Horizontal contraction 5π.) (*c*) Cross-sections of the upper side of the water-surface envelope at intervals $\epsilon t = 1{\cdot}6\pi$, in a frame of reference moving with the group velocity, for two modulation wavelengths of the modulated permanent wave, $\epsilon = 0{\cdot}1$, $\mu = 5$, $l/L = 0{\cdot}2$. (Horizontal contraction 5π.)

8. Modulated Stokes wave: recurrence obscured

The Stokes wave with parameters $\epsilon = 0{\cdot}1$, $\mu = 5$ is modulated now at 10 times the fundamental wavelength ($l/L = 0{\cdot}1$). Reference to figure 3 shows that this modulation is unstable and, further, that the second harmonic of the modulation ($l/L = 0{\cdot}2$) is also unstable. The initial growth of the modulation is therefore exponential, according to the linearized theory. The nonlinear interaction of the modulation with itself generates

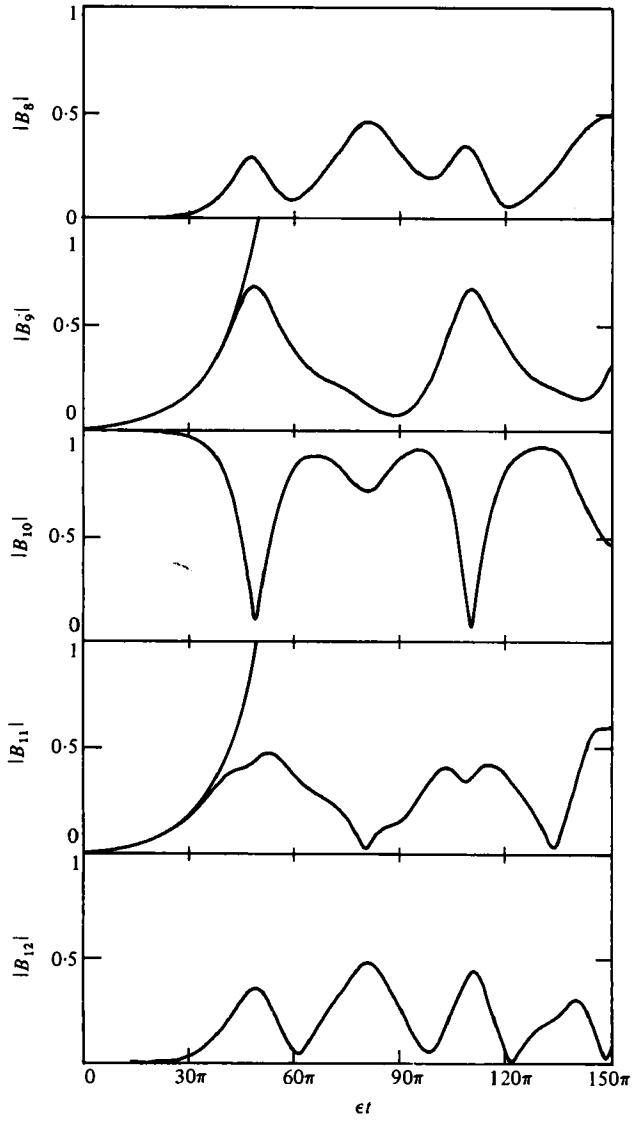

FIGURE 6 (*a*). For legend see facing page.

harmonics which themselves grow exponentially, obscuring the cyclic recurrence of the original modulation. The fundamental now has wavenumber 10, with the initial side-band modulation being applied at wavenumbers 9 and 11. The initial conditions are $B_9 = 0{\cdot}01, B_{10} = 0{\cdot}9958, B_{11} = 0{\cdot}01, B_{20} = 0{\cdot}0503, B_{30} = 0{\cdot}0041, B_k = 0$ otherwise; $1 \leqslant k \leqslant 24$, $28 \leqslant k \leqslant 32$, with $c = 1{\cdot}00497$.

The moduli of the Fourier amplitudes B_8, B_9, B_{10}, B_{11}, B_{12} are drawn in figure 6 (*a*) together with the linearized solutions calculated by the methods of § 5. The degradation in the periodic structure of B_9, B_{10}, B_{11} is seen to be associated with the initial resonant growth and subsequent oscillation of B_8 and B_{12}. The resultant structure of all 5 harmonics is a superposition of the slower cyclic structure of the central 3 harmonics and the faster cyclic structure of the outer 2 harmonics.

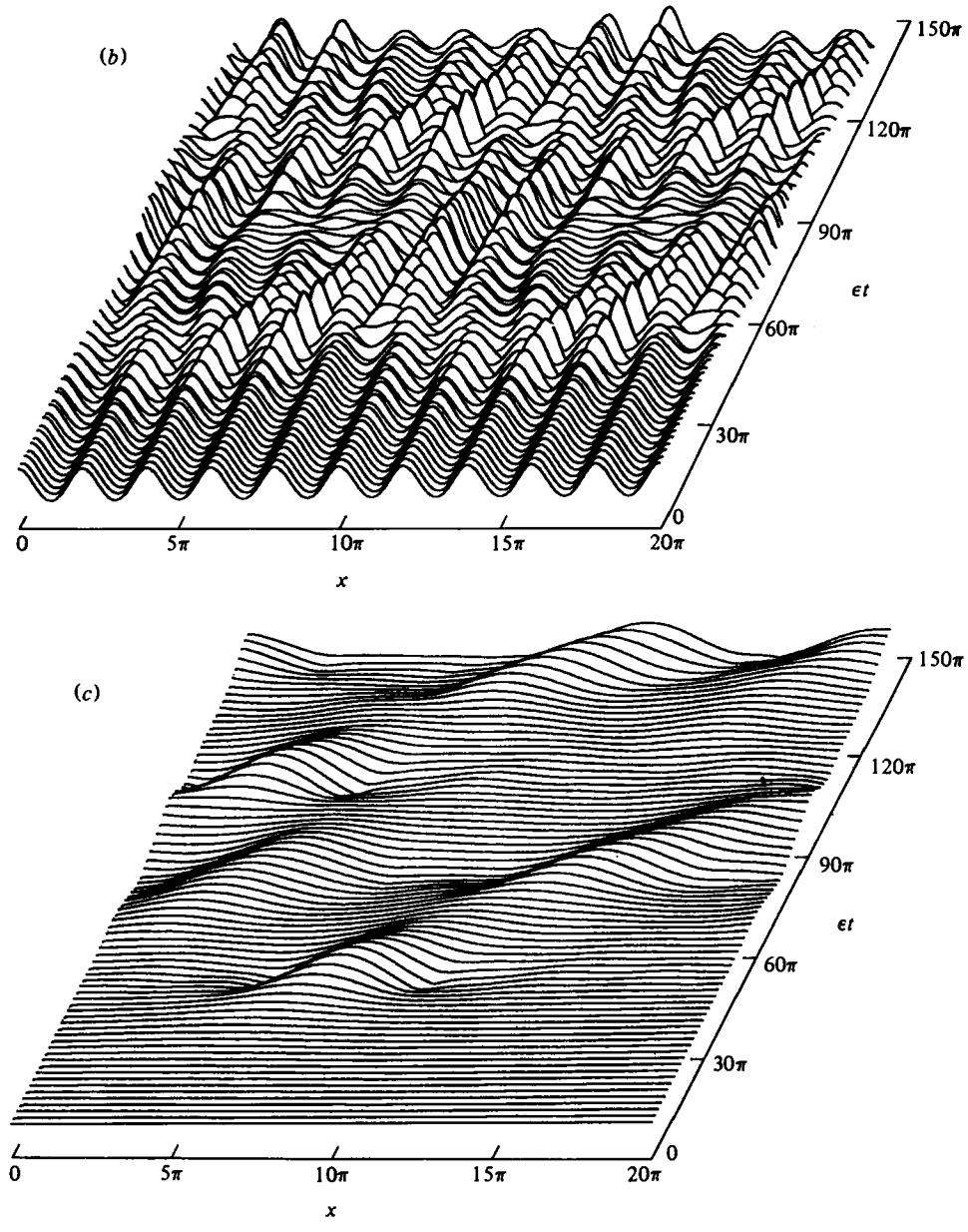

FIGURE 6. (*a*) Moduli of the Fourier amplitudes B_8, B_9, B_{10}, B_{11}, B_{12} for the modulated permanent wave, $\epsilon = 0{\cdot}1$, $\mu = 5$, $l/L = 0{\cdot}1$. The upper curves for B_9 and B_{11} are the solutions calculated by the linear-stability analysis of §5. (*b*) Cross-sections of the water-surface displacement at intervals $\epsilon t = 2\pi$, in a frame of reference moving with the wave velocity, for one modulation wavelength of the modulated permanent wave, $\epsilon = 0{\cdot}1$, $\mu = 5$, $l/L = 0{\cdot}1$. (Horizontal contraction 5π.) (*c*) Cross-sections of the upper side of the water-surface envelope at intervals $\epsilon t = 2\pi$, in a frame of reference moving with the group velocity, for one modulation wavelength of the modulated permanent wave, $\epsilon = 0{\cdot}1$, $\mu = 5$, $l/L = 0{\cdot}1$. (Horizontal contraction 5π.)

k	1	2	6	7	8	9	10
B_k	−0·0022	−0·0014	0·0015	0·0078	0·0370	0·1699	0·3820
k	11	12	13	14	15	16	17
B_k	0·2657	0·1010	0·0371	0·0129	0·0039	0·0011	0·0008
k	18	19	20	21	22	23	24
B_k	0·0026	0·0067	0·0117	0·0120	0·0084	0·0047	0·0024
k	30	31					
B_k	0·0007	0·0008					

TABLE 1

The surface displacement is illustrated in figure 6 (*b*) in a frame of reference moving with the unmodulated Stokes-wave velocity c. After the initial interval, there is a continual concentration of energy in individual crests in turn within the 10 waves of the modulation wavelength. Bearing in mind that the cross-sections in the figure are at intervals of slow time $\epsilon t = 2\pi$, the surface is similar in appearance to the ocean surface, with continual growth and decay of individual waves within a group structure.

The envelope of the surface displacement is shown in figure 6 (*c*) in a frame of reference moving with the group velocity of the fundamental harmonic $k_0 = 10$. The major ridge originates from the initial maximum modulation at $x = 0$, traverses the figure with a velocity in excess of the group velocity into the next modulation wavelength, when its successor appears on the figure as the ridge in the top-left corner. The smaller subsidiary ridge has the same spacing from the major ridge as the two ridges in figure 5 (*c*), associating it with the growth of the harmonics at wavenumbers 8 and 12. There is good agreement between the form of figure 6 (*c*) and the form of the corresponding solution of the cubic Schrödinger equation by Yuen & Ferguson (1978*a*, figure 5, case 2).

9. Modulated wave group: cyclic recurrence

The nonlinear wave group with parameters $\epsilon = 0{\cdot}1$, $\mu = 5$, $k_0 = 10$ is illustrated at the top of figure 1. It is modulated now by a perturbation of amplitude 0·01 at each of the side-band wavenumbers 9 and 11. The initial conditions are given in table 1. The parameters c and α were given the values for the unmodulated wave group, namely $c = 0{\cdot}5004$, $\alpha = 0{\cdot}2366$. The difference equations solved from these initial conditions are identical with equations (6.3) except that the coefficient of the second term is replaced by

$$\left(n\omega_{k_0} + \frac{k - nk_0}{k_0}c + n\alpha\epsilon^2 - \omega_k\right)\Big/\epsilon,$$

where $n = 0$ for $1 \leqslant k \leqslant 2$, $n = 1$ for $6 \leqslant k \leqslant 16$, $n = 2$ for $17 \leqslant k \leqslant 24$, $n = 3$ for $30 \leqslant k \leqslant 31$.

A comparison of the estimated eigenvalues for wave stability (5.2) and wave-group stability (5.3) shows that the latter are approximately a factor ϵ smaller in magnitude. The evolution of the modulated wave group above is therefore a factor ϵ slower than the evolution of a modulated wave train. This is reflected in the growth of the moduli of the Fourier amplitudes B_9, B_{10}, B_{11}, which are drawn in figure 7 as functions of $\epsilon^2 t$ rather than ϵt. The upper curve in each case is the solution found by the linear-stability

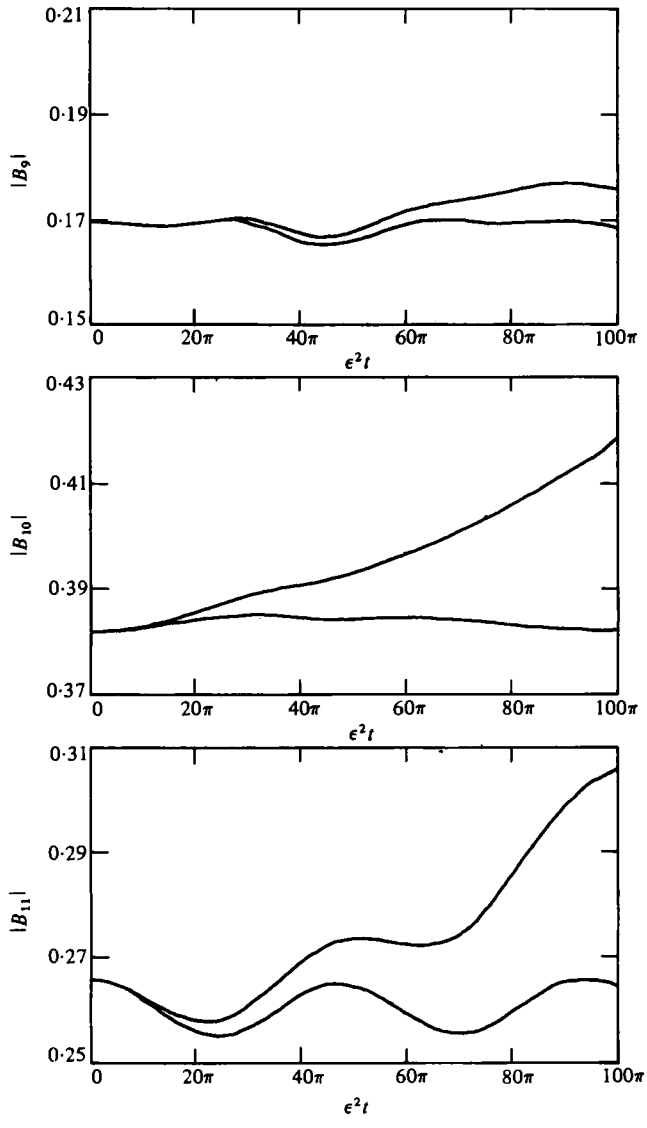

FIGURE 7. Moduli of the Fourier amplitudes B_9, B_{10}, B_{11} for the modulated nonlinear wave group $\epsilon = 0{\cdot}1$, $\mu = 5$, $k_0 = 10$, $l/L = 0{\cdot}1$. The upper curves are the solutions calculated by the linear stability analysis of §5.

analysis, and the lower curve is the solution calculated from the nonlinear evolution equations. Reasonable cyclic recurrence is found for B_{11}, the harmonic with the greatest variation. The variation in magnitude of all the harmonics is much smaller than that occurring in a modulated Stokes wave, and is too small to be detected in a sketch of the upper envelope of the surface. The amplitude of the modulation has to be increased from 1 % to 10 % of the wave group amplitude for a small oscillation of the envelope to be discernible (Bryant 1979, figure 5(*c*)).

10. Discussion

It is well known that a Stokes wave is linearly unstable to side-band modulations. At the non-dimensional depth $\mu = 5$, for example, figure 2 shows that a permanent wave of steepness $\epsilon = 0{\cdot}1$ is unstable to the side-band modulations triggered by swell for which the permanent-to-swell wavelength ratio l/L is less than about 0·24. To put it another way, if such a permanent wave has wavenumber k_0, it is unstable to all side-band modulations in the range $0{\cdot}76k_0$–$1{\cdot}24k_0$. Each pair $k_0 \pm \kappa$ within this range interacts resonantly with the permanent wave according to the mechanism described by Benjamin (1967). If swell of 20 times the wavelength of this permanent wave triggers the side-band modulations, for example, the resulting evolution of the wave train is dominated by the harmonics with wavenumbers $0{\cdot}8k_0$, $0{\cdot}85k_0$, $0{\cdot}9k_0$, $0{\cdot}95k_0$, k_0, $1{\cdot}05k_0$, $1{\cdot}1k_0$, $1{\cdot}15k_0$, $1{\cdot}2k_0$. The pair $0{\cdot}95k_0$, $1{\cdot}05k_0$ is triggered initially by the swell of wavenumber $0{\cdot}05k_0$, and all other harmonics within the range of resonance are generated by further nonlinear interactions.

The nonlinear wave group of group wavelength 20 times the central wavelength is dominated by the same 9 harmonics listed above, except that now the resonant interactions between these harmonics are in equilibrium. The side-band modulations triggered by swell now interact with harmonics which are in equilibrium, and in which the individual harmonics have smaller amplitudes than that of the fundamental in a permanent wave of the same total amplitude. In contrast with permanent waves, therefore, nonlinear wave groups are only weakly affected by swell and side-band modulation. Nonlinear wave groups tend towards permanent-wave trains in the limit of vanishing amplitude, when the difference between their side-band modulation also vanishes.

The modulation by swell of a wave train weakens on shallower water, until on water which is sufficiently shallow ($u < 1{\cdot}35$ at $\epsilon = 0{\cdot}1$) the wave train retains its form and is not converted into a group structure by swell propagating in the same direction. Nonlinear wave groups of permanent envelope flatten as the water depth decreases, until on water which is sufficiently shallow ($\mu < 1{\cdot}55$ at $\epsilon = 0{\cdot}1$) they no longer exist. It is only on deeper water that the modulation of wave trains by swell is of a magnitude to be of interest.

If the spectrum of ocean waves on deeper water is sharply peaked so that the side-band harmonics generated by swell are far from equilibrium with the central harmonic, the periodic wave train described by the sharply peaked spectrum evolves under the influence of swell into a changing group structure. During this evolution, individual waves rise for short times to larger amplitudes, during which irreversible processes such as wave breaking may occur.

This work was partially supported by a contract with the Office of Naval Research while I was a Visiting Professor at the University of California, San Diego. I am grateful to John Miles for making this visit possible.

Appendix

$$\omega_{-l} = -\omega_l \quad (l > 0).$$

$$P_{k,l} = \frac{\omega_k^2}{\omega_k + \omega_{k+l} - \omega_l}\left(\omega_l^2 + \omega_{k+l}^2 - \omega_l\omega_{k+l} - \frac{l(k+l)}{k_0^2\omega_l\omega_{k+l}}\right) - \frac{k(\omega_{k+l} - \omega_l)}{k_0^2(\omega_k + \omega_{k+l} - \omega_l)}\left(\frac{l}{\omega_l} + \frac{k+l}{\omega_{k+l}}\right).$$

$$Q_{k,l}=\frac{(\omega_{k+l}-\omega_l)\cosh(k\mu/k_0)}{\omega_k+\omega_{k+l}-\omega_l}\left(\omega_l^2+\omega_{k+l}^2-\omega_l\omega_{k+l}-\frac{l(k+l)}{k_0^2\omega_l\omega_{k+l}}\right)-\frac{k\cosh(k\mu/k_0)}{k_0^2(\omega_k+\omega_{k+l}-\omega_l)}\left(\frac{l}{\omega_l}+\frac{k+l}{\omega_{k+l}}\right).$$

$$\omega_{m-l}=-\omega_{l-m}\quad(l>m).$$

$$\begin{aligned}\bar{R}_{k,l,m}=\frac{2}{\omega_k+\omega_m+\omega_{k+l-m}-\omega_l}\Bigg[\Bigg\{&\frac{\omega_k^2}{\omega_k+\omega_{m-l}+\omega_{k+l-m}}\\
&\times\left(\omega_{m-l}^2+\omega_{k+l-m}^2+\omega_{m-l}\omega_{k+l-m}-\frac{(m-l)(k+l-m)}{k_0^2\omega_{m-l}\omega_{k+l-m}}\right)\\
&+\frac{k\omega_k}{k_0^2(\omega_{m-l}+\omega_k+\omega_{k+l-m})}\left(\frac{m-l}{\omega_{m-l}}+\frac{k+l-m}{\omega_{k+l-m}}\right)\Bigg\}\\
&\times\left\{\frac{\omega_{m-l}^2}{\omega_{m-l}+\omega_m-\omega_l}\left(\omega_l^2+\omega_m^2-\omega_l\omega_m-\frac{lm}{k_0^2\omega_l\omega_m}\right)-\frac{(m-l)(\omega_m-\omega_l)}{k_0^2(\omega_{m-l}+\omega_m-\omega_l)}\left(\frac{l}{\omega_l}+\frac{m}{\omega_m}\right)\right\}\\
&+\frac{k(m-l)}{k_0^2}\frac{\omega_m+\omega_{k+l-m}-\omega_l}{\omega_{m-l}+\omega_m-\omega_l}\left(\omega_l^2+\omega_m^2-\omega_l\omega_m-\frac{lm}{k_0^2\omega_l\omega_m}\right)\\
&+\frac{k(m-l)^2}{k_0^4\omega_{m-l}}\frac{\omega_m+\omega_{k+l-m}-\omega_l}{\omega_{m-l}+\omega_m-\omega_l}\left(\frac{l}{\omega_l}+\frac{m}{\omega_m}\right)-\omega_k^2\omega_{m-l}^2\left(\omega_l^2+\omega_m^2-\omega_l\omega_m-\frac{lm}{k_0^2\omega_l\omega_m}\right)\\
&-\omega_k^2\omega_{k+l-m}\left(1-\frac{(m-l)(k+l-m)}{k_0^2\omega_{m-l}^2\omega_{k+l-m}^2}\right)\left\{\frac{\omega_{m-l}^2}{\omega_{m-l}+\omega_m-\omega_l}\left(\omega_l^2+\omega_m^2-\omega_l\omega_m-\frac{lm}{k_0^2\omega_l\omega_m}\right)\right.\\
&\left.+\frac{m-l}{k_0^2}\left(\frac{l}{\omega_l}+\frac{m}{\omega_m}\right)\frac{\omega_{m-l}}{\omega_{m-l}+\omega_m-\omega_l}\right\}\Bigg]+\frac{1}{\omega_k+\omega_m+\omega_{k+l-m}-\omega_l}\\
&\times\left[\left\{\frac{\omega_k^2}{\omega_k+\omega_{k+l}-\omega_l}\left(\omega_l^2+\omega_{k+l}^2-\omega_l\omega_{k+l}-\frac{l(k+l)}{k_0^2\omega_l\omega_{k+l}}\right)+\frac{k\omega_k}{k_0^2(\omega_k+\omega_{k+l}-\omega_l)}\left(\frac{l}{\omega_l}+\frac{k+l}{\omega_k+l}\right)\right\}\right.\\
&\times\left\{\frac{\omega_{k+l}^2}{\omega_{k+l}+\omega_m+\omega_{k+l-m}}\left(\omega_m^2+\omega_{k+l-m}^2+\omega_m\omega_{k+l-m}-\frac{m(k+l-m)}{k_0^2\omega_m\omega_{k+l-m}}\right)\right.\\
&\left.-\frac{(k+l)(\omega_m+\omega_{k+l-m})}{k_0^2(\omega_{k+l}+\omega_m+\omega_{k+l-m})}\left(\frac{m}{\omega_m}+\frac{k+l-m}{\omega_{k+l-m}}\right)\right\}\\
&+\frac{k(k+l)}{k_0^2}\frac{\omega_m+\omega_{k+l-m}-\omega_l}{\omega_{k+l}+\omega_m+\omega_{k+l-m}}\left(\omega_m^2+\omega_{k+l-m}^2+\omega_m\omega_{k+l-m}-\frac{m(k+l-m)}{k_0^2\omega_m\omega_{k+l-m}}\right)\\
&+\frac{k(k+l)^2}{k_0^4\omega_{k+l}}\frac{\omega_m+\omega_{k+l-m}-\omega_l}{\omega_{k+l}+\omega_m+\omega_{k+l-m}}\left(\frac{m}{\omega_m}+\frac{k+l-m}{\omega_{k+l-m}}\right)-\omega_k^2\omega_{k+l}^2\\
&\times\left(\omega_m^2+\omega_{k+l-m}^2+\omega_m\omega_{k+l-m}-\frac{m(k+l-m)}{k_0^2\omega_m\omega_{k+l-m}}\right)+\omega_k^2\omega_l\left(1+\frac{l(k+l)}{k_0^2\omega_l^2\omega_{k+l}^2}\right)\\
&\times\left\{\frac{\omega_{k+l}^2}{\omega_{k+l}+\omega_m+\omega_{k+l-m}}\left(\omega_m^2+\omega_{k+l-m}^2+\omega_m\omega_{k+l-m}-\frac{m(k+l-m)}{k_0^2\omega_m\omega_{k+l-m}}\right)\right.\\
&\left.+\frac{k+l}{k_0^2}\left(\frac{m}{\omega_m}+\frac{k+l-m}{\omega_{k+l-m}}\right)\frac{\omega_{k+l}}{\omega_{k+l}+\omega_m+\omega_{k+l-m}}\right\}\\
&-\frac{k}{k_0^2}\left((\omega_m+\omega_{k+l-m}-\omega_l)(l\omega_l+m\omega_m+(k+l-m)\omega_{k+l-m})+\frac{\omega_k^2}{k_0^2}(\omega_m+\omega_{k+l-m}-\omega_l)\right.\\
&\left.\times\left(\frac{(k+l-m)^2}{\omega_{k+l-m}}+\frac{m^2}{\omega_m}-\frac{l^2}{\omega_l}\right)-\frac{2\omega_k^2}{k_0^2}\left(\frac{m(k+l-m)\omega_m}{\omega_{k+l-m}}+\frac{lm\omega_l}{\omega_m}+\frac{(k+l-m)l\omega_{k+l-m}}{\omega_l}\right)\right].\end{aligned}$$

$$R_{k,l,m}=\tfrac{1}{2}(\bar{R}_{k,l,m}+\bar{R}_{k,l,k+l-m}).$$

REFERENCES

BENJAMIN, T. B. 1967 Instability of periodic wavetrains in nonlinear dispersive systems. *Proc. R. Soc. Lond.* A **299**, 59–75.

BRYANT, P. J. 1974 Stability of periodic waves in shallow water. *J. Fluid Mech.* **66**, 81–96.

BRYANT, P. J. 1979 Nonlinear wave groups in deep water. *Stud. Appl. Math.* **61**, 1–30.

HASIMOTO, H. & ONO, H. 1972 Nonlinear modulation of gravity waves. *J. Phys. Soc. Japan* **33**, 805–811.

LAKE, B. M. & YUEN, H. C. 1978 A new model for nonlinear wind waves. Part 1. Physical model and experimental evidence. *J. Fluid Mech.* **88**, 33–62.

LAKE, B. M., YUEN, H. C., RUNGALDIER, H. & FERGUSON, W. E. 1977 Nonlinear deep water waves: theory and experiment. Part 2. Evolution of a continuous wave train. *J. Fluid Mech.* **83**, 49–74.

LONGUET-HIGGINS, M. S. 1978 The instabilities of gravity waves of finite amplitude in deep water. II. Subharmonics. *Proc. R. Soc. Lond.* A **360**, 489–505.

PHILLIPS, O. M. 1974 Wave interactions. *Nonlinear Waves* (ed. Sidney Leibovich & A. Richard Seebass), pp. 186–211. Cornell University Press.

WATSON, K. M. & WEST, B. J. 1975 A transport-equation description of nonlinear ocean surface wave interactions. *J. Fluid Mech.* **70**, 815–826.

WHITHAM, G. B. 1967 Nonlinear dispersion of water waves. *J. Fluid Mech.* **27**, 399–412.

WHITHAM, G. B. 1974 *Linear and Nonlinear Waves.* Wiley.

WILKINSON, J. H. & REINSCH, C. 1971 *Linear Algebra.* Springer.

YUEN, H. C. & FERGUSON, W. E. 1978*a* Relationship between Benjamin–Feir instability and recurrence in the nonlinear Schrödinger equation. *Phys. Fluids* **21**, 1275–1278.

YUEN, H. C. & FERGUSON, W. E. 1978*b* Fermi–Pasta–Ulam recurrence in the two-space dimensional nonlinear Schrödinger equation. *Phys. Fluids* **21**, 2116–2118.